Surface Differentiation and Localization by Parametric Modeling of Infrared Intensity Scans*

Tayfun Aytaç and Billur Barshan
Department of Electrical Engineering
Bilkent University
TR-06800 Bilkent, Ankara, Turkey
{*taytac, billur*}*@ee.bilkent.edu.tr*

***Abstract*— In this study, surfaces with different properties are differentiated with simple low-cost infrared (IR) emitters and detectors in a location-invariant manner. The intensity readings obtained from such sensors are highly dependent on the location and properties of the surface, which complicates the differentiation and localization process. Our approach, which models IR intensity scans parametrically, can distinguish different surfaces independent of their positions. The method is verified experimentally with wood, Styrofoam packaging material, white painted wall, white and black cloth, and white, brown, and violet paper. A correct differentiation rate of 100% is achieved for six surfaces and the surfaces are localized within absolute range and azimuth errors of 0.2 cm and 1.1°, respectively. The differentiation rate decreases to 86% for seven surfaces and to 73% for eight surfaces. The method demonstrated shows that simple IR sensors, when coupled with appropriate processing, can be used to differentiate different types of surfaces in a location-invariant manner.**

***Index Terms*— surface differentiation, infrared sensors, position estimation, Lambertian reflection, feature extraction**

I. Introduction

Surface differentiation and localization is of considerable interest for intelligent autonomous systems that need to explore their environment and identify different types of surfaces in a cost-effective manner. In this study, we propose the use of a simple IR sensor consisting of one emitter and one detector, where the emitted light is reflected from the target and the return intensity is measured at the detector. Although these devices are inexpensive, practical, and widely available, their use has been mostly limited to the detection of the presence or absence of objects in the environment for applications such as obstacle avoidance or counting. Gathering further information about the objects with simple IR sensors has not been much investigated. However, due to the limited resources of autonomous systems, the available resources need to be exploited as much as possible. This means that the ability of simple sensor systems to extract information about the environment should first be maximally exploited before more expensive sensing modalities with higher resolution and higher resource requirements (such as computing power) are considered for a given task. Therefore, one of the aims of this study is to explore the limits of simple and inexpensive IR sensors for surface differentiation and localization in order to extend their usage to tasks beyond simple proximity detection.

One problem with the use of simple IR detectors is that it is not possible to deduce the surface properties and the geometry of the reflecting target based on a single intensity return without knowing its position and orientation, because the reflected light depends highly on the distance and the angular orientation of the reflecting target. Similarly, one cannot make accurate range estimates based on a single intensity return. Due to single intensity readings not providing much information about an object's properties, the recognition capabilities of IR sensors have been underestimated and underused in most work. One way around this problem is to employ IR sensors in combination with other sensing modalities to acquire information about the surface properties of the object once its distance is estimated. Such an approach is taken in [1] and [2] where colors are differentiated by employing IR and ultrasonic sensors in a complementary fashion. Reference [3] is based on a similar approach where the properties of planar surfaces at a known distance (measured by an ultrasonic sensor) are determined first. Once the surface type is determined, the IR sensor is used as a range finder for the same type of surface at other distances. In this paper, we propose a scanning technique to collect intensity signals and a method for surface differentiation by parametric modeling of IR intensity scans. The proposed approach can differentiate a moderate number of surfaces and estimate their positions accurately.

IR sensors are used in robotics and automation, process control, remote sensing, and safety and security systems. More specifically, they have been used in simple object and proximity detection [4], counting, distance and depth

*This research was supported by TÜBİTAK under BDP and 197E051 grants.

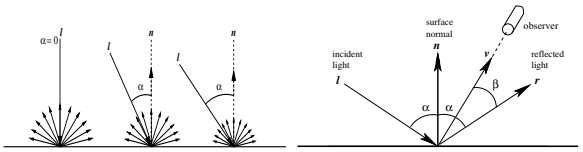

(a) (b)

Fig. 1. (a) Diffuse reflection and (b) specular reflection from an opaque surface.

monitoring, floor sensing, position measurement and control, obstacle/collision avoidance [5], and map building [6]. IR sensors are used in door detection and mapping of openings in walls [7], as well as monitoring doors/windows of buildings and vehicles, and "light curtains" for protecting an area. In our earlier works [8]–[10], we considered the differentiation and localization of objects using a template-based approach, which uses distinctive natures of the IR intensity scans. Our approach in these earlier works can be considered as non-parametric, unlike the approach taken in this paper.

II. Modeling of IR Intensity Scans

Light reflected from objects depends on the wavelength, the distance, and the properties of the light source (i.e., point or diffuse source), and the surface properties of the objects such as reflectivity, absorbtivity, transmittivity, and orientation [11]. Depending on the surface properties, reflectance can be modeled in different ways:

Matte materials can be approximated as ideal Lambertian surfaces which absorb no light and reflect all the incident light with equal intensities in all directions with respect to the cosine of the incidence angle [11]. When a Lambertian surface is illuminated by a point source of radiance $\boldsymbol{l_i}$, then the radiance reflected from the surface will be

$$\boldsymbol{l_{s,L}} = \boldsymbol{l_i}[k_d(\boldsymbol{l}.\boldsymbol{n})] \tag{1}$$

where k_d is the coefficient of the diffuse reflection for a given material and $\boldsymbol{l}$ and $\boldsymbol{n}$ are the unit vectors representing the directions of the light source and the surface normal, respectively, as shown in Figure 1(a).

In perfect or specular (mirror-like) reflection, the incident light is reflected in the plane defined by the incident light and the surface normal, making an angle with the surface normal which is equal to the incidence angle α [Fig. 1(b)].

The Phong model [12], which is frequently used in computer graphics applications to represent the intensity of energy reflected from a surface, combines the three types of reflection, which are ambient, diffuse (Lambertian), and specular reflection, in a single formula:

$$\boldsymbol{l_{s,total}} = \boldsymbol{l_a}k_a + \boldsymbol{l_i}[k_d(\boldsymbol{l}.\boldsymbol{n})] + \boldsymbol{l_i}[k_s(\boldsymbol{r}.\boldsymbol{v})^m] \tag{2}$$

where $\boldsymbol{l_{s,total}}$ is the total radiance reflected from the surface, $\boldsymbol{l_a}$ and $\boldsymbol{l_i}$ are the ambient and incident radiances on the surface, k_α, k_d, and k_s are the coefficients of ambient light, diffuse, and specular reflection for a given material, $\boldsymbol{l}$, $\boldsymbol{n}$, $\boldsymbol{r}$, and $\boldsymbol{v}$ are the unit vectors representing the directions of the light source, the surface normal, the reflected light, and the viewing angle, respectively, as shown in Figure 1(b), and m refers to the order of the specular fall-off or shine. The scalar product in the second term of the Phong model equals $\cos\alpha$, where α is the angle between the vectors $\boldsymbol{l}$ and $\boldsymbol{n}$. Similarly, the scalar product in the last term of the Phong model equals $\cos\beta$ where β is the angle between $\boldsymbol{r}$ and $\boldsymbol{v}$. Since the IR emitter and receiver are situated at approximately the same position, then the angle β between the reflected vector $\boldsymbol{r}$ and the viewing vector $\boldsymbol{v}$ is equal to 2α.

In [3], the simple non-empirical mathematical model represented by (2) is used to model reflections from planar surfaces located at a known distance (10 cm) by fitting the reflectance data to the model to improve the accuracy of the range estimates of IR sensors over a limited range interval (5–23 cm). A similar approach with a simplified reflection model is employed in [13], where an IR system can measure distances up to 1 m. The requirement of prior knowledge of the distance to the surface is eliminated in [14] by considering two angular intensity scans taken at two different known distances (10 and 12 cm). The distance error is less than 1 cm over a very limited range interval (10–18 cm) for the reflection coefficients found based on the scans at 10 and 12 cm. As the distance increases to the maximum operating range (24 cm), the distance error increases. For five different surfaces, a correct classification rate of 75% is achieved by considering the invariance property of the sum of the reflection coefficients below a certain range (14 cm).

Our approach differs from those in [3] and [13] in that it takes distance as a variable and does not require prior knowledge of the distance. Another difference is that, those works concentrate mainly on range estimation over a very limited range interval rather than the determination of the surface type, whereas in this study, we focus on the determination of the surface type over a broader range interval. When we compare our results with those of [14], we can conclude that the proposed approach is better in terms of the correct differentiation rate and the number of surfaces considered.

The surface materials considered are wood, Styrofoam packaging material, white painted wall, white and black cloth, and white, brown, and violet paper. The IR sensor [15] [Fig. 2(a)] is mounted on a 12 inch rotary table [16] to obtain angular intensity scans from these surfaces. A photograph of the experimental setup and its schematics can be seen in Figs. 2(b) and 3, respectively.

Reference intensity scans are collected for each surface

(a) (b)

Fig. 2. (a) The IR sensor used and (b) the experimental setup.

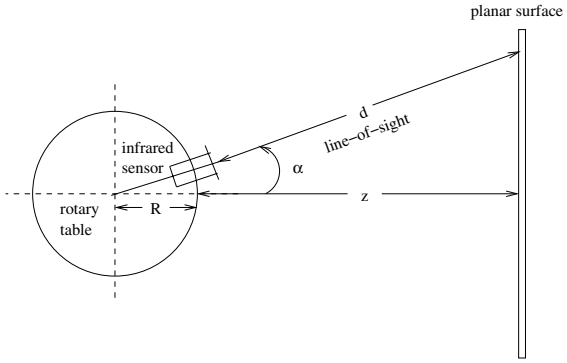

Fig. 3. Top view of the experimental setup. Both the scan angle α and the azimuth θ are measured counter-clockwise from the horizontal axis.

type by locating the surfaces between 30 to 52.5 cm with 2.5-cm distance increments, at θ=0°. The resulting reference scans for the eight surfaces are shown in Fig. 4 using dotted lines. These intensity scans have been modeled by approximating the surfaces as ideal Lambertian surfaces. The received return signal intensity is proportional to the detector area and inversely proportional to the square of the distance to the surface and is modeled with three parameters as

$$\mathcal{I} = \frac{C_0 \cos(\alpha C_1)}{\left[\frac{z}{\cos(\alpha)} + R(\frac{1}{\cos(\alpha)} - 1)\right]^2} \tag{3}$$

which is a modified version of the second term in the model represented by (2). In our case, the ambient reflection component, which corresponds to the first term in (2), can be neglected with respect to the other terms because the IR filter, covering the detector window, filters out this term. In (3), the product of the intensity of the emitter, the area of the detector, and the reflection coefficient of the surface is lumped into the constant C_0, and C_1 is an additional coefficient to compensate for the change in the basewidth of the intensity scans with respect to distance (Fig. 4). A similar dependence on C_1 is used in sensor modeling in [17]. The z is the horizontal distance between the rotary platform and the surface as shown in Fig. 3. The denominator of $\mathcal{I}$ is the square of the distance d between the IR sensor and the surface. From the geometry of Fig. 3, $d + R = \frac{z+R}{\cos(\alpha)}$, from which we obtain d as $\frac{z}{\cos(\alpha)} + R(\frac{1}{\cos(\alpha)} - 1)$, where R is the radius of the rotary platform and α is the angle made between the IR sensor and the horizontal.

Besides the model represented by (3), we tried to fit a number of other models to our experimental data, which were basically different variations of (2). The increase in the number of model parameters results in overfitting to the experimental data, whereas simpler models result in larger curve fitting errors. The model represented by (3) was the most suitable in the sense that it provided a reasonable trade-off.

Based on the model represented by (3), parameterized curves have been fitted to the reference intensity scans by using a nonlinear least-squares technique based on a model-trust region method using MATLAB™ [18]. Resulting curves are shown in Fig. 4 in solid lines. For the reference scans, z is not taken as a parameter since the distance between the surface and the IR sensing unit is already known. The initial guesses of the parameters must be made cleverly so that the algorithm does not converge to local minima and curve fitting is achieved in a smaller number of iterations. The initial guess for C_0 is made by evaluating $\mathcal{I}$ at α=0°, and corresponds to the product of $\mathcal{I}$ with z^2. Similarly, the initial guess for C_1 is made by evaluating C_1 from (3) at a known angle α other than zero, with the initial guess of C_0 and the known value of z. While curve fitting, C_0 value is allowed to vary between $\pm$ 2000 of its initial guess and C_1 is restricted to be positive. The variations of C_0, C_1, and z with respect to the maximum intensity of the reference scans are shown in Fig. 5. As the distance d decreases, the maximum intensity increases and C_0 first increases then decreases but C_1 and z both decrease, as expected from the model represented by (3). The model fit is much better for scans with smaller maximum intensities because our model takes only diffuse reflections into account, but the contribution of the specular reflection components around the maximum value of the intensity scans increases as the distance decreases. This effect can be seen in the C_0 coefficient, where C_0 value begins to decrease beyond a certain range, whose average value over all surfaces is approximately 36 cm. However, the same effect cannot be observed in the variation of C_1 [Fig. 5(b)], which is critical in our decision process. This way, the operating range of our system is extended at the expense of the error in curve fitting at smaller ranges.

III. Experimental Verification and Discussion

In this section, we experimentally verify the proposed method. In the test process, the surfaces are randomly located at azimuth angles varying from –45° to 45°, and range values between 30 to 52.5 cm. In the given region, the return signal

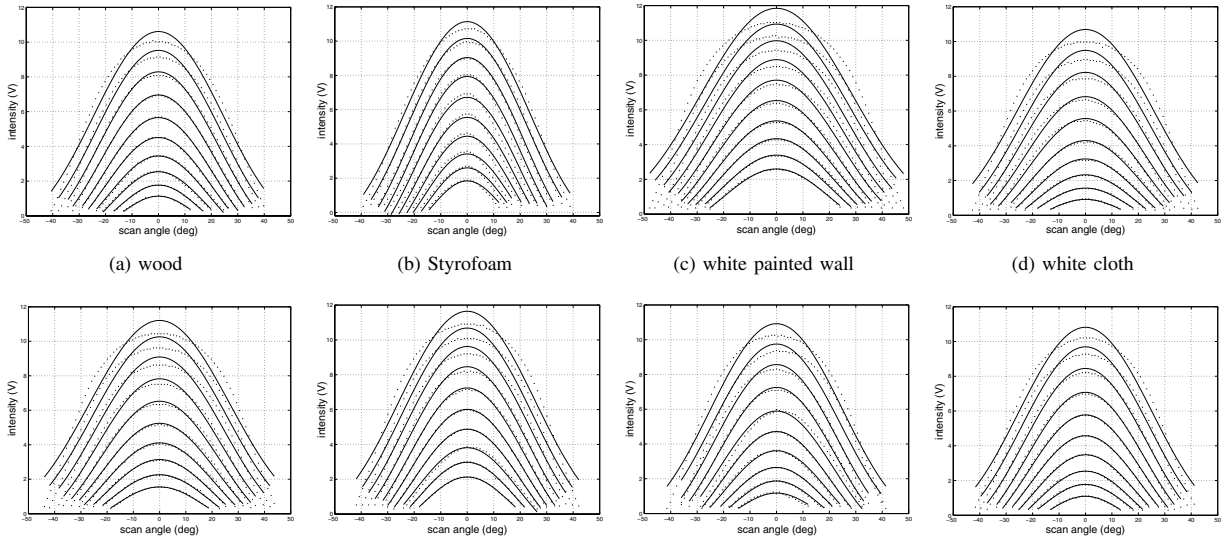

(a) wood (b) Styrofoam (c) white painted wall (d) white cloth

(e) black cloth (f) white paper (g) brown paper (h) violet paper

Fig. 4. Intensity scans of the eight surfaces collected between 30 to 52.5 cm with 2.5-cm increments. Solid lines indicate the model fit and the dotted lines indicate the actual data.

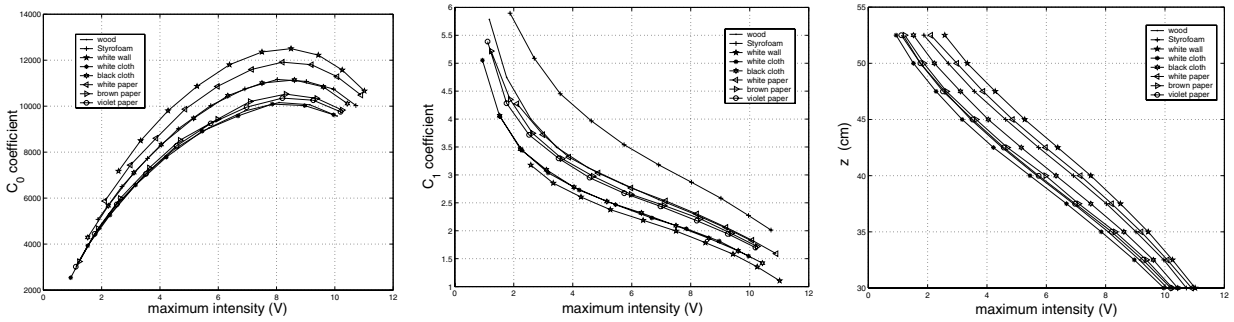

(a) (b) (c)

Fig. 5. Variations of the parameters (a) C_0, (b) C_1, and (c) z with respect to maximum intensity.

intensities do not saturate. In fact, we have experimented with fitting models to the saturated scans so that the operating range of the system is extended to include the saturation regions. However, these trials have not been very successful. For unsaturated scans, first, the maximum intensity of the observed intensity scan is found and the angular value where this maximum occurs is taken as the azimuth estimate of the surface. If there are multiple maximum intensity values, the average of the minimum and maximum angular values where the maximum intensity values occur is calculated to find the azimuth estimate of the surface. Then, the observed scan is shifted by the azimuth estimate and the model represented by (3) is fitted using a model-trust region based nonlinear least-squares technique. The initial guess for the distance z is found from Fig. 5(c) by taking the average of the maximum possible and the minimum possible range values corresponding to the maximum value of the recorded intensity scan. (Linear interpolation is used between the data points in the figure.) This results in a maximum absolute range error of approximately 2.5 cm. Therefore, the parameter z is allowed to vary between $\pm$2.5 cm of its initial guess. Using the initial guess for z, the initial guesses for C_0 and C_1 are made in the same way as explained before for the reference scans. After nonlinear curve fitting to the observed scan, we get three parameters C_0^*, C_1^*, and z^*. In the decision process, the maximum intensity of the observed scan is used and a value of C_1 is obtained by linear interpolation between the data points in Fig. 5(b) for each surface type. In other words, Fig. 5(b) is used like a look-up table. Surface-type decisions are made based on the absolute difference of $C_1 - C_1^*$ for

TABLE I

SURFACE CONFUSION MATRIX: INITIAL RANGE IS ESTIMATED USING THE MAXIMUM INTENSITY OF THE SCAN. (WO: WOOD, ST: STYROFOAM, WW: WHITE WALL, WC: WHITE CLOTH, BC: BLACK CLOTH, WP: WHITE PAPER, BR: BROWN PAPER, VI: VIOLET PAPER).

surface	differentiation result							total
	WO	ST	WW	WC/BC	WP	BR	VI	
WO	4	–	–	–	7	–	1	12
ST	–	12	–	–	–	–	–	12
WW	–	–	12	–	–	–	–	12
WC/BC	–	–	–	12	–	–	–	12
WP	4	–	–	–	8	–	–	12
BR	–	–	–	–	–	12	–	12
VI	–	–	–	–	–	–	12	12
total	8	12	12	12	15	12	13	84

each surface because of the more distinctive nature of the C_1 variation with respect to the maximum intensity. The surface type giving the minimum difference is chosen as the correct one. The decision could have also been made by comparing the parameters with those at the estimated range. However, this would not give better results because of the error and the uncertainty in the range estimates. We have also considered taking different combinations of the differences $C_0 - C_0^*$, $C_1 - C_1^*$, and $z - z^*$ as our error criterion. However, the criterion based on $C_1 - C_1^*$ difference was the most successful.

The best differentiation results are achieved for a set of surfaces including Styrofoam packaging material, white painted wall, white or black cloth, and white, brown, and violet paper. We get a correct differentiation rate of 100% for these six surfaces and the surfaces are located with absolute range and azimuth errors of 0.2 cm and 1.1°, respectively. We can increase the number of surfaces differentiated at the expense of a decrease in the correct differentiation rate. For example, if we add wood to our test set keeping either white or black cloth, we get a correct differentiation rate of 86% for seven surfaces (Table I). For these sets of surfaces, absolute position errors are 0.6 cm and 1.1°. Similarly, if we form a set of surfaces excluding wood but keeping both white and black cloth, we achieve a correct differentiation rate of 83% for seven surfaces (Table II) and the surfaces are located with absolute position errors of 0.5 cm and 1.1°. The differentiation results for all eight surfaces considered are tabulated in Table III. Over these eight surfaces, an overall correct differentiation rate of 73% is achieved and surfaces are located with absolute position errors of 0.8 cm and 1.1°. In the estimation results, note that the range estimation accuracy improves with increasing correct classification rate, whereas the azimuth estimation accuracy is independent of it, as expected. In the last case, white and black cloth as well as wood and white paper are surface pairs mostly confused with each other.

TABLE II

SURFACE CONFUSION MATRIX: INITIAL RANGE IS ESTIMATED USING THE MAXIMUM INTENSITY OF THE SCAN.

surface	differentiation result							total
	ST	WW	WC	BC	WP	BR	VI	
ST	12	–	–	–	–	–	–	12
WW	–	12	–	–	–	–	–	12
WC	–	–	7	5	–	–	–	12
BC	–	–	9	3	–	–	–	12
WP	–	–	–	–	12	–	–	12
BR	–	–	–	–	–	12	–	12
VI	–	–	–	–	–	–	12	12
total	12	12	16	8	12	12	12	84

TABLE III

SURFACE CONFUSION MATRIX: INITIAL RANGE IS ESTIMATED USING THE MAXIMUM INTENSITY OF THE SCAN.

surface	differentiation result								total
	WO	ST	WW	WC	BC	WP	BR	VI	
WO	4	–	–	–	–	7	–	1	12
ST	–	12	–	–	–	–	–	–	12
WW	–	–	12	–	–	–	–	–	12
WC	–	–	–	7	5	–	–	–	12
BC	–	–	–	9	3	–	–	–	12
WP	4	–	–	–	–	8	–	–	12
BR	–	–	–	–	–	–	12	–	12
VI	–	–	–	–	–	–	–	12	12
total	8	12	12	16	8	15	12	13	96

To investigate the effect of the initial range estimate of the surface on the differentiation process, we now assume that the distance to the surface is known beforehand. For this case, only the two variables C_0 and C_1 are taken as parameters. For the same six surfaces considered as in the previous case (where the initial range to the surface is estimated using the maximum intensity of the scan), the same correct classification rate of 100% is achieved. If we add wood to our test set keeping either white or black cloth, we get a correct differentiation rate of 87% for seven surfaces (see Ref. [19] for the detailed results). Similarly, if we form a set of surfaces excluding wood but keeping both white and black cloth, we achieve a correct differentiation rate of 88% for seven surfaces. The differentiation result over all eight surfaces is 78%. When we compare these results with those obtained without exact knowledge of the distance to the surface, we can conclude that similar surfaces are confused with each other (wood/white paper and white/black cloth) with smaller confusion rates.

IV. Conclusion

The main accomplishment of this study is that we achieved position-invariant surface differentiation and localization with simple IR sensors despite the fact that their individual intensity readings are highly dependent on the surface position and properties, and this dependence cannot be represented by a simple analytical relationship. The intensity scan data acquired from a simple low-cost IR emitter and detector pair was processed and modeled. Different parameterized reflection models were considered and evaluated to find the most suitable model fit to our experimental data which also best represents and classifies the surfaces under consideration. The proposed approach can differentiate six different surfaces with 100% accuracy. In [9], where we considered differentiation and localization of surfaces by employing non-parametric approaches, a maximum correct differentiation rate of 87% over four surfaces was achieved. Comparing this rate with that obtained in this study, we can conclude that the parametric approach is superior to non-parametric ones, in terms of the accuracy, number of surfaces differentiated, and memory requirements, since the non-parametric approaches we considered require the storage of reference scan signals. By parameterizing the intensity scans and storing only their parameters, we have eliminated the need to store complete reference scans.

This work demonstrates that simple IR sensors, when coupled with appropriate processing, can be used to extract substantially more information about the environment than such devices are commonly employed for. We expect this flexibility to significantly extend the range of applications in which such low-cost single sensor based systems can be used. Specifically, we expect that it will be possible to go beyond relatively simple tasks such as simple object and proximity detection, counting, distance and depth monitoring, floor sensing, position measurement, obstacle/collision avoidance, and deal with tasks such as differentiation, classification, recognition, clustering, position estimation, map building, perception of the environment and surroundings, autonomous navigation, and target tracking. The approach presented here would be more useful where self-correcting operation is possible due to repeated observations and feedback.

The demonstrated system would find application in intelligent autonomous systems such as mobile robots whose task involves surveying an unknown environment made of different surface types. Current and future work involves designing a more intelligent system whose operating range is adjustable based on an initial range estimate to the surface. This will eliminate saturation and allow the system to accurately differentiate and localize surfaces over a wider operating range. Another issue we are considering is the extension of the model to include specular reflections from glossy surfaces. We are also working on the recognition of surfaces through the use of artificial neural networks in order to improve the accuracy. Parametric modeling and representation of intensity scans of different geometries is also being considered to employ the proposed approach in the simultaneous determination of the geometry and the surface type of targets.

References

[1] V. Genovese, E. Guglielmelli, A. Mantuano, G. Ratti, A. M. Sabatini, and P. Dario, "Low-cost, redundant proximity sensor system for spatial sensing and color-perception," *Electronics Letters*, vol. 31, no. 8, 13 April 1995, pp. 632–633.

[2] A. M. Sabatini, V. Genovese, E. Guglielmelli, A. Mantuano, G. Ratti, and P. Dario, "A low-cost composite sensor array combining ultrasonic and infrared proximity sensors," in *Proc. IROS*, vol. 3, pp. 120–126, Pittsburgh, PA, 5–9 August 1995.

[3] P. M. Novotny and N. J. Ferrier, "Using infrared sensors and the Phong illumination model to measure distances," in *Proc. ICRA*, pp. 1644–1649, Detroit, MI, 10–15 May 1999.

[4] E. Cheung and V. J. Lumelsky, "Proximity sensing in robot manipulator motion planning: system and implementation issues," *IEEE Trans. Robot. Automat.*, vol. 5, pp. 740–751, Dec. 1989.

[5] V. J. Lumelsky and E. Cheung, "Real-time collision avoidance in teleoperated whole-sensitive robot arm manipulators," *IEEE Trans. Syst. Man Cybern.*, vol. 23, pp. 194–203, Jan./Feb. 1993.

[6] H. -H. Kim, Y. -S. Ha, and G. -G. Jin, "A study on the environmental map building for a mobile robot using infrared range-finder sensors," in *Proc. IROS*, pp. 716–711, Las Vegas, NV, 27–31 Oct. 2003.

[7] A. M. Flynn, "Combining sonar and infrared sensors for mobile robot navigation," *Int. J. Robot. Res.*, vol. 7, pp. 5–14, Dec. 1988.

[8] T. Aytaç and B. Barshan, "Differentiation and localization of targets using infrared sensors," in *Proc. IROS*, pp. 105–110, Lausanne, Switzerland, Oct. 2002.

[9] B. Barshan and T. Aytaç, "Position-invariant surface recognition and localization using infrared sensors," *Opt. Eng.*, vol. 42, pp. 3589–3594, Dec. 2003.

[10] T. Aytaç and B. Barshan, "Simultaneous extraction of geometry and surface properties of targets using simple infrared sensors," *Opt. Eng.*, vol. 43, pp. 2437–2447, Oct. 2004.

[11] S. K. Nayar, K. Ikeuchi, and T. Kanade, "Surface reflection: Physical and geometrical perspectives," *IEEE Trans. Pattern Anal. Mach. Intell.*, vol. 13, pp. 611–634, July 1991.

[12] B. T. Phong, "Illumination for computer generated pictures," *Commun. ACM*, vol. 18, pp. 311–317, June 1975.

[13] G. Benet, F. Blanes, J. E. Simó, and P. Pérez, "Using infrared sensors for distance measurement in mobile robots," *Robot. Autonom. Syst.*, vol. 40, pp. 255–266, Sep. 2002.

[14] M. A. Garcia and A. Solanas, "Estimation of distance to planar surfaces and type of material with infrared sensors," in *Proc. ICPR*, Cambridge, UK, 23–26 Aug. 2004.

[15] Matrix Elektronik, AG, Kirchweg 24 CH-5422 Oberehrendingen, Switzerland, *IRS-U-4A Proximity Switch Datasheet*, 1995.

[16] Arrick Robotics, P.O. Box 1574, Hurst, Texas, 76053 URL: www.robotics.com/rt12.html, *RT-12 Rotary Positioning Table*, 2002.

[17] G. Petryk and M. Buehler, "Dynamic object localization via a proximity sensor network," in *Proc. IROS*, pp. 337–341, Washington D.C., 8–11 Dec. 1996.

[18] T. Coleman, M. A. Branch, and A. Grace, *MATLAB Optimization Toolbox, User's Guide*, 1999.

[19] T. Aytaç and B. Barshan, "Surface differentiation by parametric modeling of infrared intensity scans," to appear in *Opt. Eng.*, vol. 44, pp. xxx–xxx, June 2005.